Hindawi Publishing Corporation
Journal of Nanomaterials
Volume 2015, Article ID 801606, 7 pages
http://dx.doi.org/10.1155/2015/801606

Research Article

Effects of Nitrogen-Doped Multiwall Carbon Nanotubes on Murine Fibroblasts

J. G. Munguía-Lopez,[1] E. Muñoz-Sandoval,[2] J. Ortiz-Medina,[2,3] F. J. Rodriguez-Macias,[4] and A. De Leon-Rodriguez[1]

[1]*Molecular Biology Division, Instituto Potosino de Investigación Científica y Tecnológica (IPICYT), Camino a la Presa San José 2055, Colonia Lomas 4a Sección, 78216 San Luis Potosí, SLP, Mexico*
[2]*Advanced Materials Department, Instituto Potosino de Investigación Científica y Tecnológica (IPICYT), Camino a la Presa San José 2055, Colonia Lomas 4a Sección, 78216 San Luis Potosí, SLP, Mexico*
[3]*Research Center for Exotic Nanocarbons (JST), Shinshu University, Wakasato 4-17-1, Nagano 380-8553, Japan*
[4]*Department of Fundamental Chemistry, Universidade Federal de Pernambuco, Avenida Proessor Luiz Freire, 50740-540 Recife, PE, Brazil*

Correspondence should be addressed to A. De Leon-Rodriguez; aleonr@ipicyt.edu.mx

Received 13 July 2015; Accepted 11 August 2015

Academic Editor: Faik Oktar

The effect of nitrogen-doped multiwall carbon nanotubes (CN_x) on the proliferation of NIH-3T3 murine fibroblasts is presented. CNTs were dispersed in distillated water and incubated with mammalian cells in order to evaluate their toxicity. Also, the influence of factors such as dosage (7 and 70 μg/mL), exposure time (24 to 96 h), and the exposure route (before and after cell liftoff) on the cell proliferation was evaluated. When the CN_x were simultaneously incubated with the cells, the control culture reached a maximum cell concentration of $1.3 \times 10^5 \pm 3.4 \times 10^4$ cells per well at 96 h, whereas cultures with 7 μg/mL reached a concentration of $2.6 \times 10^4 \pm 5.3 \times 10^3$ cells. In the case of 70 μg/mL of CN_x most of the cells were dead. The CN_x that were added 24 h after cell dissociation showed that live cells decreased, with a cell concentration of $9.6 \times 10^4 \pm 9 \times 10^3$ for 7 μg/mL and $5.5 \times 10^4 \pm 9.5 \times 10^3$ for 70 μg/mL, in contrast to control cultures with $1.1 \times 10^6 \pm 1.5 \times 10^4$. The results showed that the CN_x had cytotoxic effects depending on the concentration and exposure route.

1. Introduction

A wide range of nanomaterials has been developed for several applications over the past few years. Due to their physical, chemical, electrical, and thermal properties, and since their discovery in 1991 [1], carbon nanotubes (CNTs) have shown a potential for use in drug delivery, biosensor, antimicrobial nanocomposite film, and cellular scaffolding. CNTs are tiny hollow cylinders, made from a single, double, or several layers of graphene that are concentrically arranged and capped by fullerene hemispheres. They have diameters ranging from 0.4 to 2 nm for single walled carbon nanotubes (SWCNTs) and from 2 to 200 nm for multiwall carbon nanotubes (MWCNTs), and lengths ranging from hundreds of nanometers to micrometers [1–3]. Since CNTs have an asbestos-like shape, research into their toxicity and potential risks to human health has been intensified [4–7].

Studies on cellular response in nonfunctionalized or functionalized (addition of functional groups on a graphite surface) MWCNT have been extensive. Chemical doping (carbon atoms substitution) with nitrogen of CNTs (CN_x) was suggested to have positive effects on mice survival [8] and showed an improvement in cell-adhesion strength, viability, and proliferation of mammalian cells [3, 9], in contrast with the MWCNT. However, cytotoxic effects of CN_x have also been reported, where long length CN_x were more toxic than other functionalized CNTs [10]. Researches have demonstrated that cells exhibited variable responses to CNTs depending on different factors such as the method of synthesis, impurities, length and diameter, type (pristine,

functionalized, and doped), degree of dispersion/agglomeration, dispersant, CNT concentration, time exposure, cellular type, and protein adsorption [2, 5, 6, 8, 11, 12]. Due to the inconsistency in CN_x biocompatibility, more studies regarding cell response to these nanomaterials are necessary.

In the body, cell motility and wound healing are carried out by cell detachment, which is generated by proteolytic processes using endogenous proteases [13]. One of the most common enzymatic methods used for cell detachment in adherent-cell-subculture is trypsinization; trypsin cuts adhesion proteins to yield disaggregated cells with a rounded appearance. Although many cells are able to tolerate trypsin digestion during a short period of time, trypsinization causes cell stress affecting cytoskeleton proteins that are involved in regulating cell adhesion, stability, and elasticity [14–16].

CNTs have the capacity to adsorb a wide range of proteins, especially those rich in histidine, tryptophan, and phenylalanine [12], and also adhesion proteins from extracellular matrix (fibronectins, collagen) and transmembrane-proteins (integrins) [17]. Since enzymatic cell detachment can produce residual fragments of adhesion proteins, these fragments could interact with CNTs altering the extracellular matrix metabolism which is regulated by a complex mechanism including cell-cell and cell-matrix interactions [13, 17]. For this reason, the knowledge of cell-CNTs interactions is essential for cell scaffold development that is used in tissue regeneration.

The aim of this study was to evaluate the possible toxic effect of CN_x on NIH-3T3 murine fibroblast stressed by enzymatic detachment and nonstressed cells, in which a natural cell detachment stress was simulated by a trypsin incubation during a short period of time. Exposure route was defined in this work as the way to add nanomaterials to cell cultures (stressed and nonstressed cells). Besides several parameters are required to determine if new materials are safe for biomedical use; the effects of CN_x concentration and exposure time were also evaluated.

2. Materials and Methods

2.1. Synthesis, Purification, and Characterization of CN_x. In this way, CN_x were synthesized by using the chemical vapor deposition (CVD) method. As a chemical precursor 2.5 wt% ferrocene in benzylamine was used; the solution was placed into a reservoir and atomized. The aerosol was carried by an Argon flow at 2.5 L/min into a quartz tube 100 cm in length, placed inside of two tubular furnaces heated at 850°C. After 30 min of synthesis, the quartz tube was then cooled at room temperature and the CN_x were collected by internal scraping. Then, the pristine CN_x were purified and dispersed by using a pulsed probe sonicator in water under reflux, followed by a reflux in 6 M HCl and filtration.

Consequently, the purified CN_x were analyzed by scanning electron microscopy (SEM) as follows: first, the nanomaterials were pounded into a whole powder and separated into equal portions. Then, each portion was loaded into pins and visualized by SEM (Philips-XL 30 SFEG; Dual Beam (FIB/SEM) FEI-Helios Nanolab 600 equipped with an EDX detector) to determine lengths, diameters, and chemical composition of CN_x. Raman characterization was performed using a laser of 633 nm in Raman Renishaw Micro-Raman equipment.

2.2. Preparation of Dispersion of Purified CN_x. Stocks of purified CN_x were dispersed in distillated water at 1 mg/mL. Then, the samples were sonicated by an ultrasonic bath at 42 kHz and 100 W (Branson 2510 Ultrasonic Cleaner), at 40°C for 8 h, having as a result stable dispersions; these conditions were strong enough to obtain no visible agglomerates of purified CN_x. Finally, all the stocks were stored at 4°C until further use.

2.3. Cytotoxicity Assays. The effects of purified CN_x on the viability of NIH-3T3 murine fibroblast were evaluated by using the Trypan-blue exclusion method. Briefly, the cells were defrosted and cultured in a basal-IMDM (Iscove's Modified Dulbecco's Medium, SIGMA) at pH 7.2 and supplemented with 10% fetal bovine serum (GIBCO), 100 U/mL penicillin, 100 μg/mL streptomycin, and 0.25 μg/mL amphotericin B (SIGMA), using 24-well plates (Corning) over a period of 72 h in a humidity chamber at 37°C and CO_2 5% (Shell-Lab). After three passes, when 80% of cellular confluence was reached, the cells were washed twice gently with PBS (pH 7.2) and then harvested by incubation with trypsin-EDTA (0.25%-1X, GIBCO) for 10 min. Cell suspensions with a density of 2×10^3 cells per well were added into 96-well plates in absence or presence of purified CN_x at final concentrations of 7 and 70 μg/mL. For exposure route experiments, purified CN_x were added (1) immediately after cell dissociation (stressed cells) or (2) fibroblasts were firstly incubated for 24 h and then purified CN_x were added into each well (nonstressed cells). Samples were washed twice gently with PBS, incubated with trypsin for 6 min, and cells were counted by using the Trypan-blue method. During the 96 h of exposure with the nanomaterial, samples were taken each 24 h. NIH-3T3 cell cultures without nanomaterials were used as control. To avoid variation on purified CN_x concentration in cell cultures when medium was changed, kinetics were carried out using a working volume of 250 μL without medium replacement.

2.4. Statistics. The data is presented as the mean ± standard deviation, with a statistical comparison of one- and two-way ANOVA. We used Dunnett's posttests to compare treatments with control groups, and p values <0.05 were considered significant. All experiments were done in triplicate.

3. Results and Discussion

3.1. Determination of Length and Diameter of Purified CN_x. Figure 1 shows SEM micrographs and size distribution of purified CN_x. Micrographs by the XL30 and Helios are shown in Figures 1(a) and 1(c), respectively. A few bundles were found in purified CN_x samples to determine the lengths of nanomaterials (Figure 1(a)). The length range was 10 to 130 μm, being the most abundant lengths of 40–50 μm (Figure 1(b)). In micrographs of purified CN_x, the nanomaterials seemed to have similar diameters (Figure 1(c)), but, after

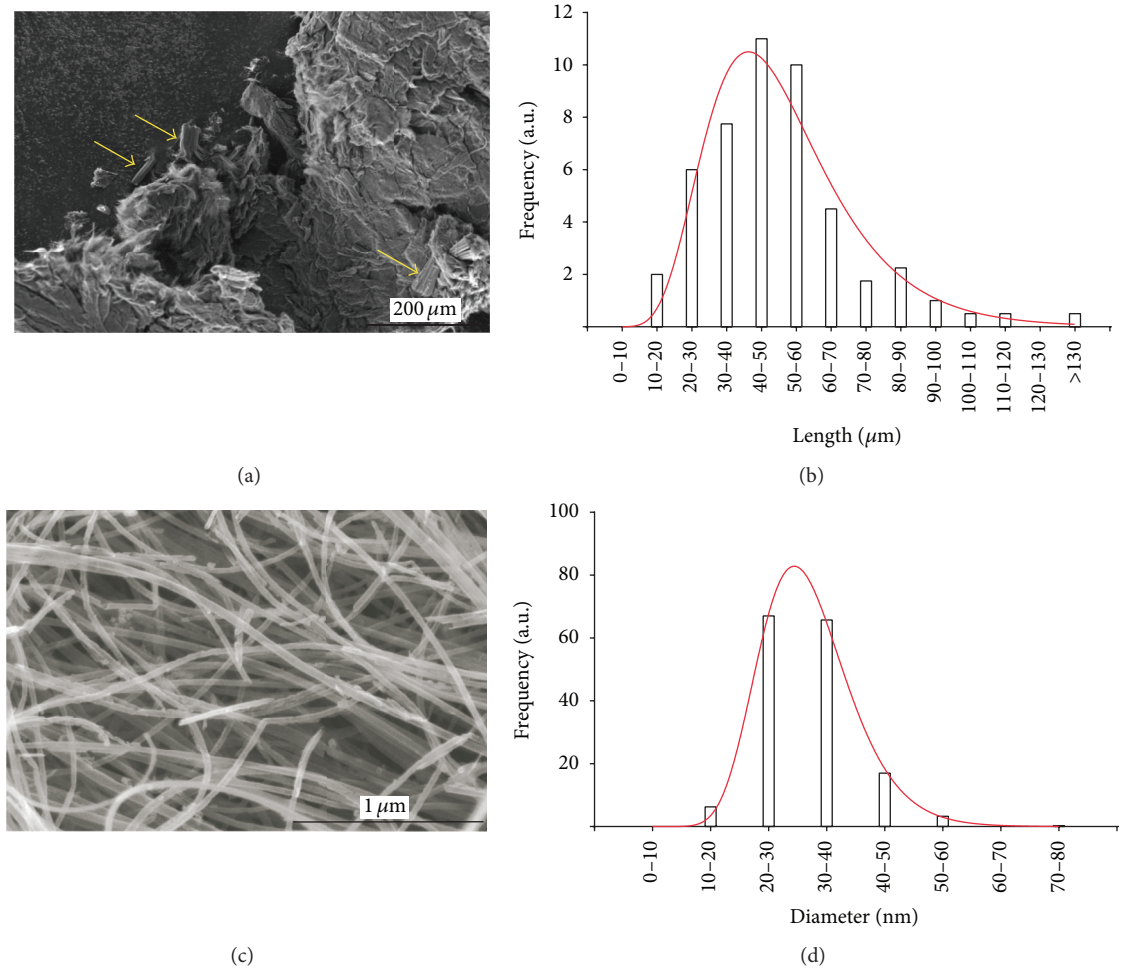

Figure 1: SEM micrographs of CN_x morphology and size distribution. Lengths were obtained from bundles of purified CN_x ((a), pointed with yellow arrows) and plotted to generate distribution patterns. Diameters were obtained from individual tubes from Helios SEM images (c) and distribution was plotted (d).

an analysis with the Helios microscopy, the diameter sizes were around 10–80 nm, with a diameter predominance of 20–40 nm (Figure 1(d)).

Nanomaterial sizes were obtained from their own bundles and short "fibrous" structures (Figure 2). The number of bundles among different samples of purified CN_x was small (around 38 bundles) (Figures 2(a)–2(c), yellow arrows), as well as in between the same sample (Figures 2(d)–2(f)). Since purified CN_x samples were mostly agglomerated in big structures by dry process, the determination of their total lengths was difficult; thus only the bundles lengths were reported. The presence of amino groups in the CN_x could be the reason to find less bundles in samples, due to their weaker van der Waals interactions, resulting in lower formation of bundles [8].

3.2. Raman and EDX Characterization of Pristine and Purified CN_x. Figure 3 shows the Raman spectra of pristine and purified CN_x plotted between 100 and 3000 cm^{-1}. The bands D (defect mode), G (graphite mode), and G′ (second order mode) situated at 1340, 1592, and 2686 cm^{-1}, respectively, are the typical peaks corresponding to carbonaceous materials. In the case of purified CN_x, the shifting to higher frequencies of G band suggests that nitrogen doping decreased. The I_D/I_G values were 1.1488 and 1.2815 for pristine and purified CN_x, respectively. This increasing in I_D/I_G ratio has been suggested as an evidence for sidewall functionalization of CNTs [18, 19].

With respect to chemical composition of our CN_x (pristine and purified), EDX analysis was carried out. Figures S1 and S2 (see Supplementary Material available online at http://dx.doi.org/10.1155/2015/801606) show the SEM images and their respective EDX graphs. The average quantity of iron in pristine samples was of 2.22 wt% (Figure S1), which decreased after purification process to 0.61 wt% (Figure S2), indicating the elimination of this contaminant (see Supplementary Material for the quantities of carbon, nitrogen, and oxygen elements).

3.3. Effect of Purified CN_x on Murine Fibroblasts Nonstressed and Stressed. 3T3 murine fibroblasts were used as a model for stromal cells, which can be found in matrix and connective tissue throughout the body. Figure 4 shows the kinetics of

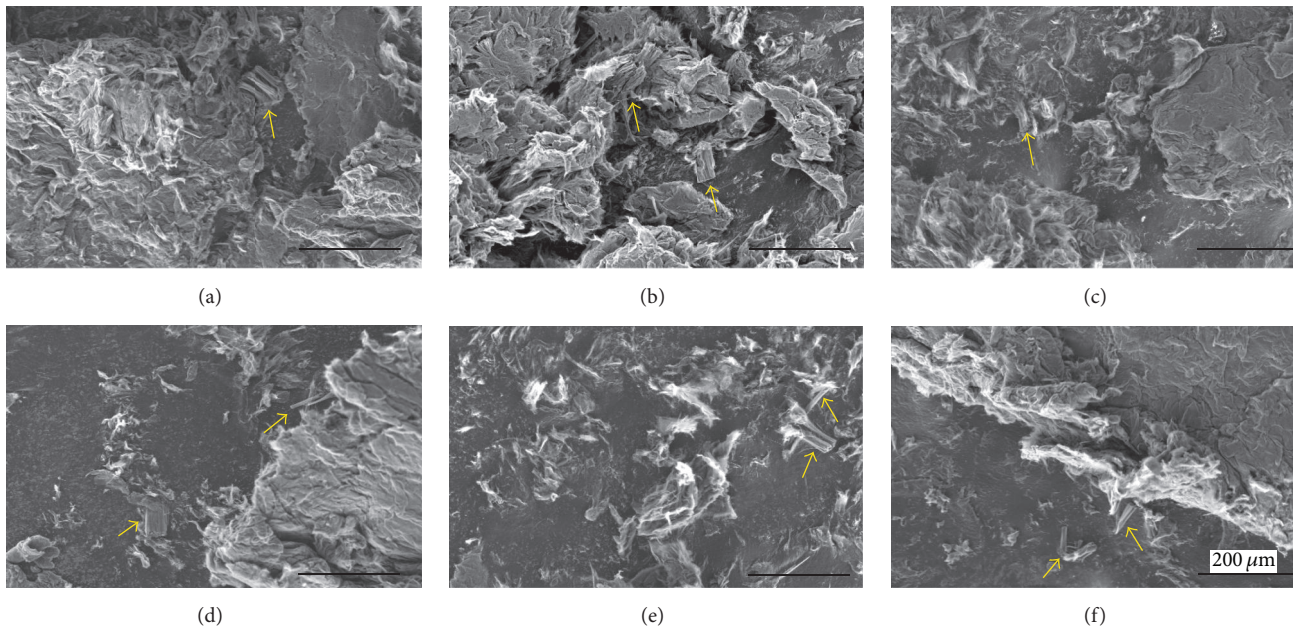

FIGURE 2: Representative SEM images of whole sample dry purified CN_x. (a–c) Different parts of sample from whole sample; (d–f) the same sample different fields. Yellow arrows pointed to bundles of purified CN_x. Big structures are agglomerates of CNTs which were easy to disperse in water.

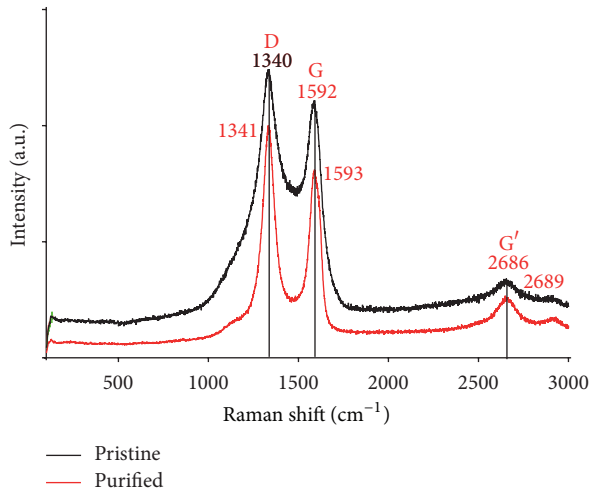

FIGURE 3: Raman spectra of pristine and purified CN_x at 633 nm.

fibroblasts growth with water-dispersed purified CN_x. When the cells were incubated simultaneously with the purified CN_x, the control culture (without purified CN_x) reached a maximum live cell concentration of $1.3 \times 10^5 \pm 3.4 \times 10^4$ cells per well at 96 h; meanwhile cultures with 7 μg/mL reached $2.6 \times 10^4 \pm 5.3 \times 10^3$ cells, and a drastic no cell survival was at 70 μg/mL of purified CN_x (Figure 4(a)). Purified CN_x added after 24 h of cell dissociation showed a decreased live cell, with a cell concentration of $9.6 \times 10^4 \pm 9 \times 10^3$ for 7 μg/mL and $5.5 \times 10^4 \pm 9.5 \times 10^3$ for 70 μg/mL, compared to control culture with $1.1 \times 10^6 \pm 1.5 \times 10^4$, at 96 h of exposure (Figure 4(b)). Results suggest that nanomaterials exhibited toxic effects, in concentration and exposure route-dependent manner. No effects concerning time exposure were observed.

Murine fibroblasts were susceptible to purified CN_x in concentration and exposure route-dependent manner. As previously mentioned, toxicity/biocompatibility of CNTs (SWCNT, MWCNT, and functionalized CNTs) on mammalian cells depends on different factors [6, 20, 21]. A lot of data research has shown the toxicity of CNTs [22–25] in human mesenchymal stem cells [26], 3T3 L1 fibroblasts [27], 3T3 fibroblast, telomerase, immortalized human bronchiolar epithelial cells, RAW 264.7 macrophages [6], mouse fibroblast cell L929, and mouse adipose-derived stem cells [3], but, to our knowledge, no experiments about the effects of CNTs have been reported on mammalian cells stressed by enzymatic detachment, which is a natural process in the body. Treatments with water-dispersed purified CN_x immediately added after cell liftoff (stressed cells by trypsin) were more toxic than purified CN_x added after 24 h of cell dissociation, suggesting that exposure route factor had negative effects on cell proliferation. This could have been caused by interaction of CNTs with residual fragments of adhesion proteins generated after cell trypsinization [12], which can still adversely affect cytoskeleton proteins that are involved in regulating cell adhesion, stability, and elasticity [14–16, 28]. However, in this work, only the cell proliferation was evaluated as a first approach to determine the purified CN_x toxicity; therefore, more studies are required and are currently underway.

Specific growth rate (μ) was calculated from exponential growth phase of fibroblasts and used as a parameter to evaluate the effect of purified CN_x on cell growth. In 7 μg/mL of dispersed-water purified CN_x incubated simultaneously with cells, μ was lower ($0.031 \pm 0.004\ h^{-1}$) than control cultivation

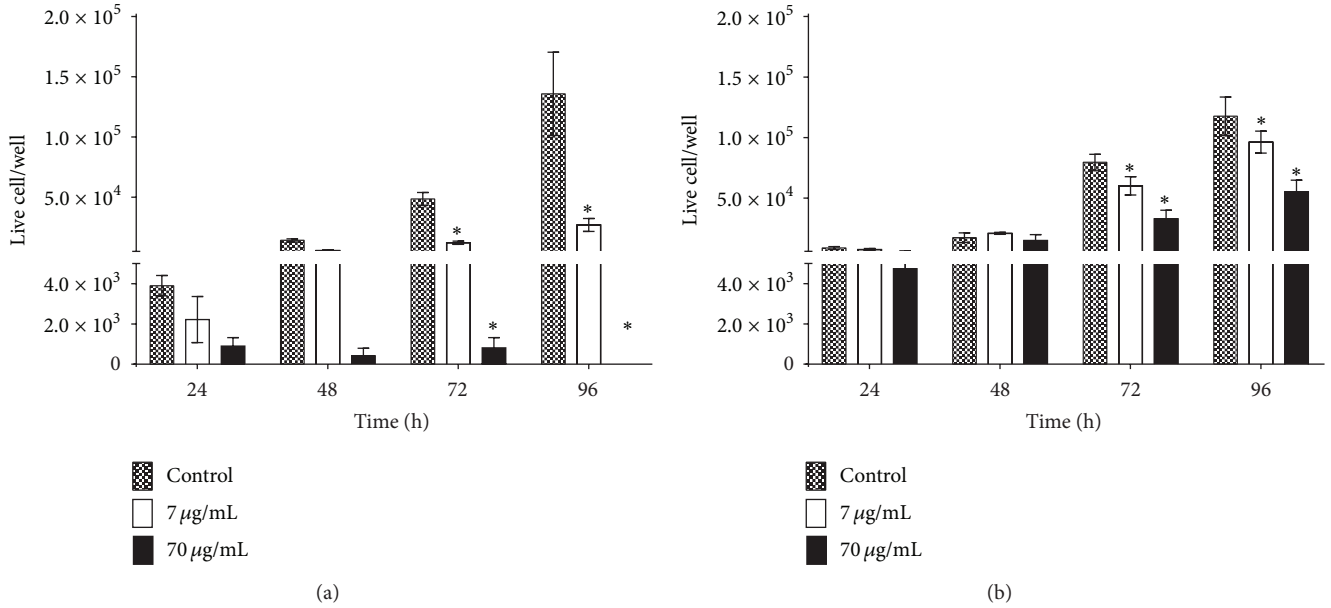

FIGURE 4: Effects of water-dispersed purified CN_x on NIH-3T3 murine fibroblast proliferation. Purified CN_x were incubated with fibroblast immediately after cell dissociation (a) or 24 h after cellular liftoff (b). Data are presented as mean ± SD. ∗ indicates significant difference compared to untreated controls ($p < 0.05$); $n \geq 3$.

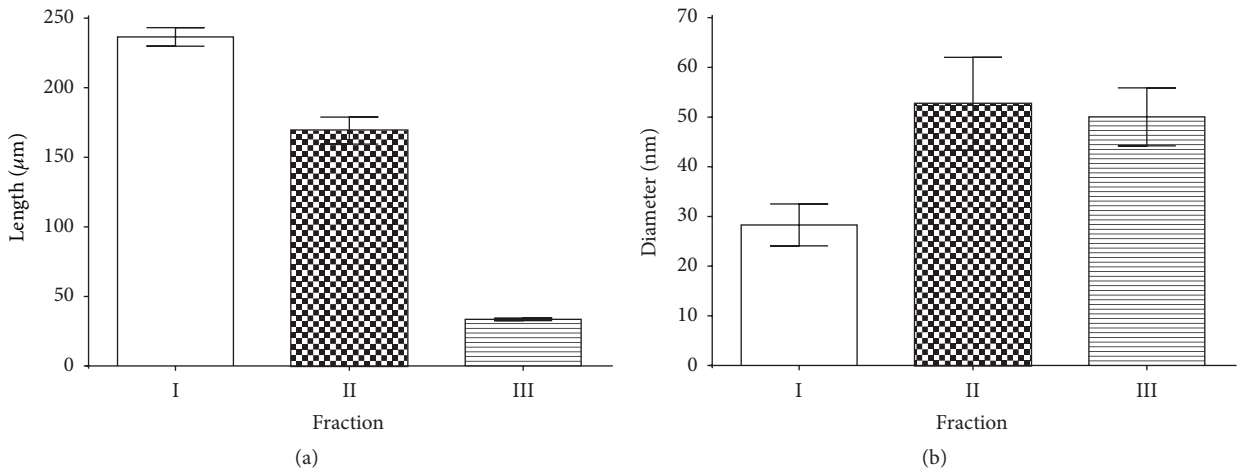

FIGURE 5: Variations in pristine CN_x length (a) and diameters (b) obtained from three different fractions of the same batch.

($0.048 \pm 0.004\ h^{-1}$); since no cells survived at 70 μg/mL, μ was not determined. Concerning incubation of cells with nanomaterials for 24 h after cell liftoff, values of μ were $0.044 \pm 0.002\ h^{-1}$ for control culture and $0.037 \pm 0.002\ h^{-1}$ and $0.035 \pm 0.001\ h^{-1}$ for purified CN_x at 7 and 70 μg/mL, respectively; both concentrations affected negatively μ. Results confirm a cytotoxic effect that is concentration and exposure route dependent.

3.4. Morphology Diversity of Pristine CN_x. In several investigations about cytotoxic effects of CNTs, these nanomaterials are purchased from companies, which are synthesized by CVD. However, researchers have reported different patterns in the bulk growth of CNTs during their synthesis, showing that the CVD method produces a wide range of CNTs morphologies with varieties of lengths and diameters [29]. In preliminary results, different fractions from the same batch were analyzed by SEM showing a wide collection of pristine CN_x sizes (Figure 5), with lengths of range between 30 and 250 μm (Figure 5(a)) and diameters of 24–60 nm (Figure 5(b)). Figure 6 shows a SEM micrograph gallery of the morphology of the different pristine CN_x fractions, where the variations in lengths (Figures 6(a)–6(c)) and diameters (Figures 6(d)–6(f)) among three fractions are clear. The morphology variation of CNTs could be the reason behind having contradictory results regarding cytotoxicity/biocompatibility of CNTs reported in several researches, and this issue should be studied in order to understand the relationship between CNTs and mammalian cell response.

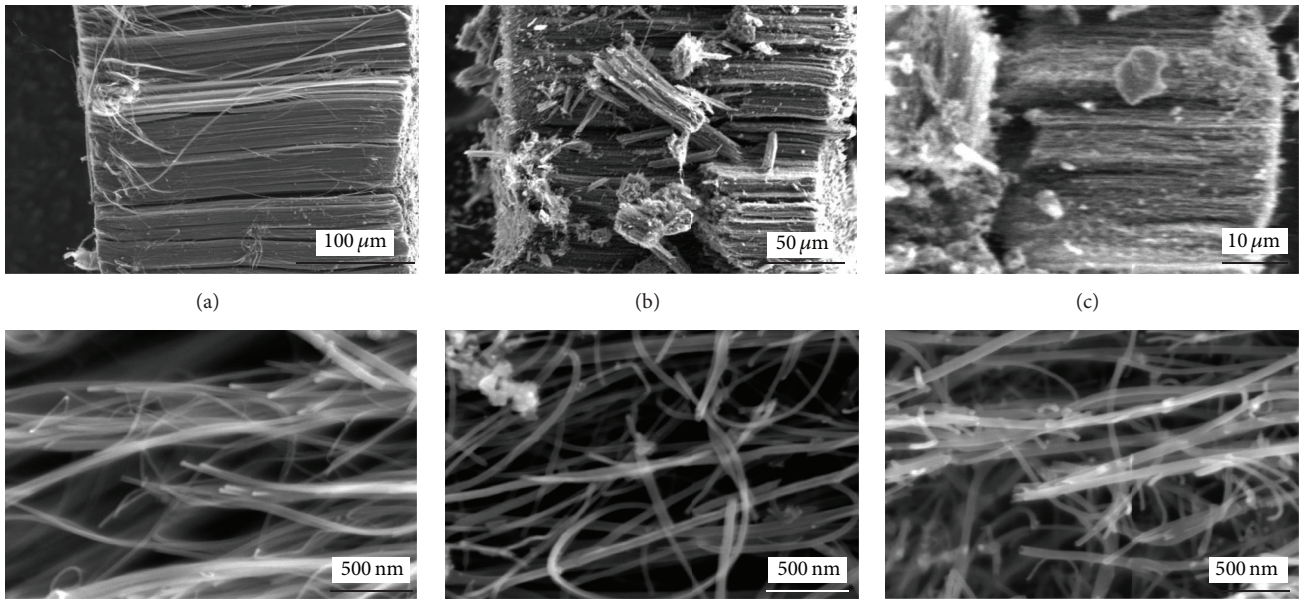

FIGURE 6: Electron micrograph gallery depicting the size diversity of pristine CN_x found in three different locations (fractions) from the quartz tube. Fractions: I (a, d), II (b, e), and III (c, f). Lengths (a–c) and diameters (d–f) of CN_x.

4. Conclusion

Finally, purified CN_x have a cytotoxicity effect that is directly dependent on their concentration; also purified CN_x showed a more toxic effect in enzymatic stressed cells than in the non-stressed ones. Since cells in the body are exposed to enzymatic processes of detachment, the present study of the effects on overstressed cells by enzymatic digestion is important for the development and potential uses of these nanomaterials in the biomedical field. On the other hand, chemical synthesis of pristine CN_x yields heterogenic product with substantial differences on length and diameter size, which have distinctive cytotoxic effects on the proliferation of NIH-3T3 cells. There is still a long path that we must take in order to understand the relationship between nanomaterials and mammalian cells. However, concentrations up to 7 μg/mL of nanotubes are well tolerated by the cells, and they could be used in biomedical applications.

Conflict of Interests

The authors declare that there is no conflict of interests regarding the publication of this paper.

Acknowledgments

The authors thank the Marcos Moshinsky Foundation and CONACYT-Mexico Grants 107082 (JFRM), CB-2013-220744 (EMS) for partial funding. J. Gil Munguía-López thanks CONACYT for its Scholarship 250279. They also thank L. Aldana for the English review and L. Ordoñez, B. A. Rivera-Escoto, and G. J. Labrada-Delgado for their technical assistance.

References

[1] S. Iijima, "Helical microtubules of graphitic carbon," *Nature*, vol. 354, no. 6348, pp. 56–58, 1991.

[2] H.-F. Cui, S. K. Vashist, K. Al-Rubeaan, J. H. T. Luong, and F.-S. Sheu, "Interfacing carbon nanotubes with living mammalian cells and cytotoxicity issues," *Chemical Research in Toxicology*, vol. 23, no. 7, pp. 1131–1147, 2010.

[3] M. L. Zhao, D. J. Li, L. Yuan, Y. C. Yue, H. Liu, and X. Sun, "Differences in cytocompatibility and hemocompatibility between carbon nanotubes and nitrogen-doped carbon nanotubes," *Carbon*, vol. 49, no. 9, pp. 3125–3133, 2011.

[4] X. Wang, T. Xia, M. C. Duch et al., "Pluronic F108 coating decreases the lung fibrosis potential of multiwall carbon nanotubes by reducing lysosomal injury," *Nano Letters*, vol. 12, no. 6, pp. 3050–3061, 2012.

[5] H. Haniu, N. Saito, Y. Matsuda et al., "Effect of dispersants of multi-walled carbon nanotubes on cellular uptake and biological responses," *International Journal of Nanomedicine*, vol. 6, pp. 3295–3307, 2011.

[6] S. K. Sohaebuddin, P. T. Thevenot, D. Baker, J. W. Eaton, and L. Tang, "Nanomaterial cytotoxicity is composition, size, and cell type dependent," *Particle and Fibre Toxicology*, vol. 7, article 22, 2010.

[7] A. Kunzmann, B. Andersson, T. Thurnherr, H. Krug, A. Scheynius, and B. Fadeel, "Toxicology of engineered nanomaterials: focus on biocompatibility, biodistribution and biodegradation," *Biochimica et Biophysica Acta (BBA)—General Subjects*, vol. 1810, no. 3, pp. 361–373, 2011.

[8] J. C. Carrero-Sánchez, A. L. Elías, R. Mancilla et al., "Biocompatibility and toxicological studies of carbon nanotubes doped with nitrogen," *Nano Letters*, vol. 6, no. 8, pp. 1609–1616, 2006.

[9] D. J. Li and L. F. Niu, "Influence of N atomic percentages on cell attachment for CNx coatings," *Bulletin of Materials Science*, vol. 26, no. 4, pp. 371–375, 2003.

[10] S. Boncel, K. H. Müller, J. N. Skepper, K. Z. Walczak, and K. K. K. Koziol, "Tunable chemistry and morphology of multi-wall carbon nanotubes as a route to non-toxic, theranostic systems," *Biomaterials*, vol. 32, no. 30, pp. 7677–7686, 2011.

[11] D. Li, L. Yuan, Y. Yang et al., "Adsorption and adhesion of blood proteins and fibroblasts on multi-wall carbon nanotubes," *Science in China, Series C: Life Sciences*, vol. 52, no. 5, pp. 479–482, 2009.

[12] X. Cai, R. Ramalingam, H. S. Wong et al., "Characterization of carbon nanotube protein corona by using quantitative proteomics," *Nanomedicine: Nanotechnology, Biology, and Medicine*, vol. 9, no. 5, pp. 583–593, 2013.

[13] R. J. McAnulty, "Fibroblasts and myofibroblasts: their source, function and role in disease," *International Journal of Biochemistry & Cell Biology*, vol. 39, no. 4, pp. 666–671, 2007.

[14] Q. Zheng, S. M. Iqbal, and Y. Wan, "Cell detachment: post-isolation challenges," *Biotechnology Advances*, vol. 31, no. 8, pp. 1664–1675, 2013.

[15] H. E. Canavan, X. Cheng, D. J. Graham, B. D. Ratner, and D. G. Castner, "Cell sheet detachment affects the extracellular matrix: a surface science study comparing thermal liftoff, enzymatic, and mechanical methods," *Journal of Biomedical Materials Research—Part A*, vol. 75, no. 1, pp. 1–13, 2005.

[16] H.-L. Huang, H.-W. Hsing, T.-C. Lai et al., "Trypsin-induced proteome alteration during cell subculture in mammalian cells," *Journal of Biomedical Science*, vol. 17, no. 1, article 36, 2010.

[17] J.-P. Kaiser, T. Buerki-Thurnherr, and P. Wick, "Influence of single walled carbon nanotubes at subtoxical concentrations on cell adhesion and other cell parameters of human epithelial cells," *Journal of King Saud University—Science*, vol. 25, no. 1, pp. 15–27, 2013.

[18] S. Lee, J.-W. Peng, and C.-H. Liu, "Raman study of carbon nanotube purification using atmospheric pressure plasma," *Carbon*, vol. 46, no. 15, pp. 2124–2132, 2008.

[19] S. Banerjee and S. S. Wong, "Rational sidewall functionalization and purification of single-walled carbon nanotubes by solution-phase ozonolysis," *The Journal of Physical Chemistry B*, vol. 106, no. 47, pp. 12144–12151, 2002.

[20] L. Meng, A. Jiang, R. Chen et al., "Inhibitory effects of multiwall carbon nanotubes with high iron impurity on viability and neuronal differentiation in cultured PC12 cells," *Toxicology*, vol. 313, no. 1, pp. 49–58, 2013.

[21] P. M. V. Raja, J. Connolley, G. P. Ganesan et al., "Impact of carbon nanotube exposure, dosage and aggregation on smooth muscle cells," *Toxicology Letters*, vol. 169, no. 1, pp. 51–63, 2007.

[22] C. L. Ursini, D. Cavallo, A. M. Fresegna et al., "Comparative cyto-genotoxicity assessment of functionalized and pristine multiwalled carbon nanotubes on human lung epithelial cells," *Toxicology in Vitro*, vol. 26, no. 6, pp. 831–840, 2012.

[23] M. Bottini, S. Bruckner, K. Nika et al., "Multi-walled carbon nanotubes induce T lymphocyte apoptosis," *Toxicology Letters*, vol. 160, no. 2, pp. 121–126, 2006.

[24] D. Liu, C. Yi, D. Zhang, J. Zhang, and M. Yang, "Inhibition of proliferation and differentiation of mesenchymal stem cells by carboxylated carbon nanotubes," *ACS Nano*, vol. 4, no. 4, pp. 2185–2195, 2010.

[25] F. A. Witzmann and N. A. Monteiro-Riviere, "Multi-walled carbon nanotube exposure alters protein expression in human keratinocytes," *Nanomedicine: Nanotechnology, Biology, and Medicine*, vol. 2, no. 3, pp. 158–168, 2006.

[26] E. Mooney, P. Dockery, U. Greiser, M. Murphy, and V. Barron, "Carbon nanotubes and mesenchymal stem cells: biocompatibility, proliferation and differentiation," *Nano Letters*, vol. 8, no. 8, pp. 2137–2143, 2008.

[27] J. Meng, M. Yang, L. Song et al., "Concentration control of carbon nanotubes in aqueous solution and its influence on the growth behavior of fibroblasts," *Colloids and Surfaces B: Biointerfaces*, vol. 71, no. 1, pp. 148–153, 2009.

[28] R. Umegaki, M. Kino-Oka, and M. Taya, "Assessment of cell detachment and growth potential of human keratinocyte based on observed changes in individual cell area during trypsinization," *Biochemical Engineering Journal*, vol. 17, no. 1, pp. 49–55, 2004.

[29] S. S. Meysami, F. Dillon, A. A. Koós, Z. Aslam, and N. Grobert, "Aerosol-assisted chemical vapour deposition synthesis of multi-wall carbon nanotubes: I. Mapping the reactor," *Carbon*, vol. 58, pp. 151–158, 2013.